

M. WOJTASZEK\*, T. ŚLEBODA\*, A. CZULAK\*\*, G. WEBER\*\*, W.A. HUFENBACH\*\*

## QUASI-STATIC AND DYNAMIC TENSILE PROPERTIES OF Ti-6Al-4V ALLOY

### WŁASNOŚCI MECHANICZNE STOPU Ti-6Al-4V W QUASI-STATYCZNYCH ORAZ DYNAMICZNYCH WARUNKACH ODKSZTAŁCENIA

Ti-6Al-4V alloy is widely used, mainly in aircraft industry, due to its low density, excellent corrosion/oxidation resistance and attractive mechanical properties. This alloy has relatively low formability, so forming parts of complex geometries out of this alloy requires precisely controlled thermomechanical processing parameters. In industrial conditions Ti-6Al-4V alloy is usually processed by forging or extrusion. Ti-6Al-4V alloy is applied for structural parts of aircrafts, which are often exposed to variable loads and high or cyclically changing strain rates. Moreover, Ti-6Al-4V alloy is often used for structural parts providing good ballistic performance. That is why the knowledge of the mechanical behaviour of this alloy under dynamic conditions is important. This work is aimed at the analysis of Ti-6Al-4V alloy behaviour under quasi-static and dynamic deformation conditions. Both dynamic and quasi-static tensile tests were performed in this research. Moreover, ARAMIS system, a non-contact and material independent measuring system providing accurate 2D displacements, surface strain values and strain rates, was applied. The influence of tensile test strain rate on chosen mechanical properties of the investigated alloy was also discussed. The investigations showed a significant influence of processing strain rate on the mechanical behaviour of Ti-6Al-4V alloy.

*Keywords:* Titanium alloy, Mechanical behaviour, Quasi-static conditions, Dynamic conditions, Tensile tests

Stop Ti-6Al-4V jest szeroko stosowany głównie w przemyśle lotniczym ze względu na niski ciężar właściwy, dużą odporność na korozję oraz wysokie własności mechaniczne. Ze względu na stosunkowo małą podatność do odkształceń plastycznych stopu Ti-6Al-4V, kształtowanie części o skomplikowanej geometrii z tego stopu wymaga bardzo dokładnego doboru warunków przeróbki cieplno-mechanicznej. W warunkach przemysłowych stop ten jest najczęściej kształtowany w procesach kucia lub wyciskania, które charakteryzują się różnymi zakresami prędkości odkształcania wsadu. Zastosowanie stopu Ti-6Al-4V obejmuje w dużej mierze wytwarzanie odpowiedzialnych elementów konstrukcji lotniczych, które są ekspozowane na zmienne obciążenia w warunkach wysokich lub cyklicznie zmiennych prędkości, oraz które często muszą charakteryzować się doskonałymi parametrami balistycznymi. Dlatego istotna w przypadku przedmiotowego materiału jest znajomość charakterystyk jego zachowania w warunkach obciążeń dynamicznych. Zauważyć można, że w odróżnieniu od danych otrzymanych w statycznych warunkach, ilość publikowanych informacji na ten temat jest niewielka. W pracy przeprowadzono próby jednoosiowego rozciągania próbek ze stopu Ti-6Al-4V, które prowadzono przy dużych prędkościach odkształcania oraz, celem porównania, w warunkach quasi-statycznych. Do analizy wykorzystano system do bezkontaktowych trójwymiarowych pomiarów odkształceń ARAMIS. Badano wpływ prędkości odkształcania na wybrane własności mechaniczne stopu, obserwacji i analizie poddano także powstałe podczas realizacji próby rozciągania powierzchnie zniszczenia.

## 1. Introduction

Ti-6Al-4V alloy is the most widely used titanium alloy due to its attractive specific strength and corrosion resistance [1]. The mechanical properties of this alloy are dictated by the initial microstructure and thermomechanical loading history. Many research works were focused on development of microstructure of this alloy during thermomechanical processing [2, 3] or on the influence of the initial microstructure of Ti-6Al-4V alloy on its processing [4-6]. The evolution of the microstructure of this alloy resulting from dynamic recrystal-

lization or dynamic recovery occurring during hot deformation was also widely discussed [7-11].

Ti-6Al-4V titanium alloy is also used for armor materials for military vehicles what requires excellent ballistic performance. Ballistic performance is known to correlate with dynamic deformation behaviour as well as the formation of adiabatic shear bands, but information on the dynamic deformation behaviour of the Ti-6Al-4V alloy is quite limited. An adiabatic shear band is a narrow region of highly localized plastic deformation, and is often observed when materials are deformed at high strain rates such as ballis-

\* AGH UNIVERSITY OF SCIENCE AND TECHNOLOGY, FACULTY OF METALS ENGINEERING AND INDUSTRIAL COMPUTER SCIENCE, AL. A. MICKIEWICZA 30, 30-059 KRAKÓW, POLAND

\*\* TECHNISCHE UNIVERSITÄT DRESDEN, INSTITUTE OF LIGHTWEIGHT ENGINEERING AND POLYMER TECHNOLOGY (ILK)

tic impact, machining, and high-speed deformation processing.

This work discusses quasi-static and dynamic tensile properties of Ti-6Al-4V alloy.

## 2. Material under investigation

Ti-6Al-4V alloy bar with a diameter of 50 mm was used as a starting material for this research. The microstructure of as-delivered alloy, consisting of  $\alpha$  and  $\beta$  phases, is shown in Fig. 1.

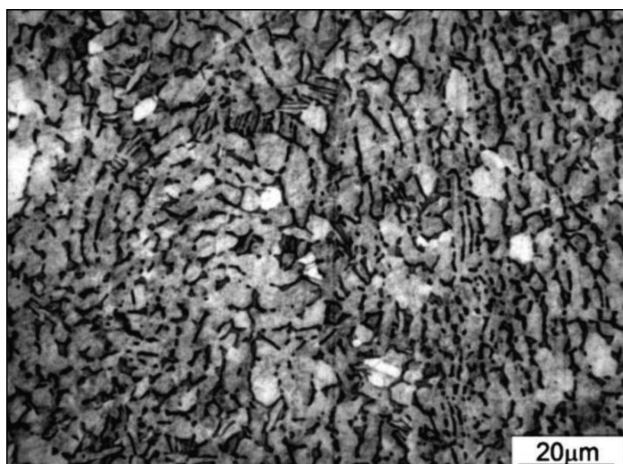


Fig. 1. Microstructure of as-received Ti-6Al-4V alloy

The chemical composition of the investigated alloy is given in Table 1.

TABLE 1

Chemical composition (weight %) of Ti-6Al-4V alloy

Ti	Al	V	Fe	C	Mo	Cr	O	N	H
Bal.	6.52	4.17	0.16	0.013	0.03	0.01	0.17	0.006	0.0011

## 3. Experimental procedure

Plate tensile specimens were cut out from the investigated Ti-6Al-4V alloy by EDM (electro-discharge machining) and then the surfaces were carefully ground to about 1,5 mm deep using abrasive paper. Finally, the specimens were polished to remove surface scratches. At last, a grey scale pattern was applied on the surface of the specimens to realize the measurement of strains by means of grey scale correlation software.

A tensile specimen is shown in Fig. 2, where also the dimensions in mm and the gauge length with applied grey scale pattern are displayed.

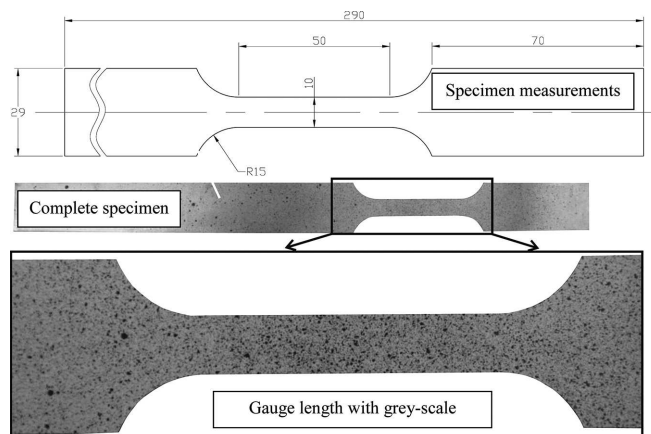


Fig. 2. Tensile specimen used for static and dynamic tensile tests with grey scale pattern applied

For the investigations and the characterisation of materials at high loading speeds a servohydraulic high velocity test system (SHP) INSTRON VHS 160/20 (Fig. 3) has been used at ILK.

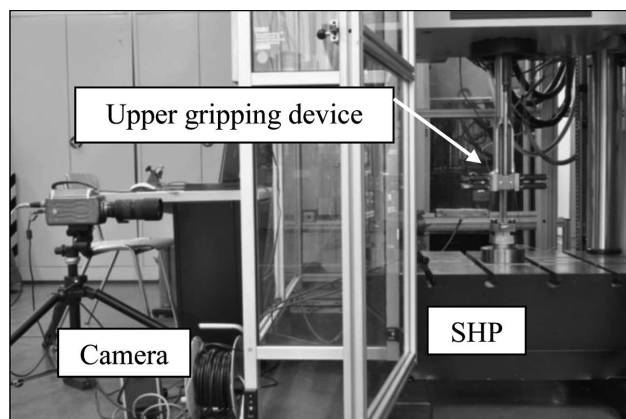


Fig. 3. Tensile testing device Instron VHS 160/20 with high speed camera Phantom v7.2

Special adaptations of the test equipment allow highly-dynamic tensile, compression and shear tests. The SHP enables tests of materials and components at high deformation speeds of up to  $20 \text{ m}\cdot\text{s}^{-1}$  and a maximum force of 160 kN [12]. The testing machine has a specially designed upper gripping device for gripping the tensile specimen at a defined testing speed. This design guarantees initial acceleration of the grip without loading of the specimen. After achieving the test velocity, spacers are pushed out and the upper clamp grabs the specimen [13]. The function of the upper gripping device is shown schematically in Figure 4 [14].

Quasi-static and dynamic tensile tests were conducted at room temperature with testing speeds of  $0.0001 \text{ m}\cdot\text{s}^{-1}$ ;  $0.1 \text{ m}\cdot\text{s}^{-1}$  and  $1 \text{ m}\cdot\text{s}^{-1}$ . The reaction force is recorded with a Kistler 9017A, 400 kN piezoelectric load washer, mechanically preset at 200 kN [14].

For means of strain determination a high speed camera Phantom v. 7.2 in combination with the grey-scale-correlation software ARAMIS was implied. This high speed camera is capable of taking up to 190.000 pictures per second. For the performed tensile tests, frame rates varied from 10 Hz at the testing speed  $0.0001 \text{ m}\cdot\text{s}^{-1}$  and 50.000 Hz at  $1 \text{ m}\cdot\text{s}^{-1}$ .

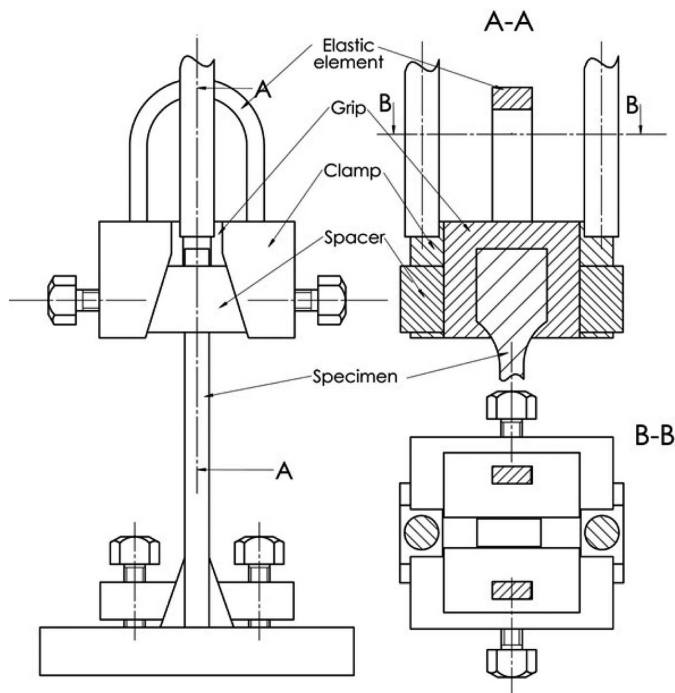


Fig. 4. Schematic upper gripping device of tensile testing machine [14]

In the present research, ARAMIS system, available at ILK, was used to determine the tensile strain of each specimen. ARAMIS is a non-contact and material independent measuring system, providing accurate 2D displacements, surface strain values (major and minor strain) and strain rates for statically or dynamically loaded test objects. The ARAMIS system determines the grey scale distribution of the surface of the investigated object and calculates the displacements and strains of this distribution between each picture taken by the digital high speed camera Phantom v. 7.2.

Graphical representation of the calculated data allows observing and interpreting the mechanical behaviour of the investigated object.

The results and the method of calculation of tensile strains by the ARAMIS software during a tensile test with  $0.1 \text{ m}\cdot\text{s}^{-1}$  is shown in Figure 5.

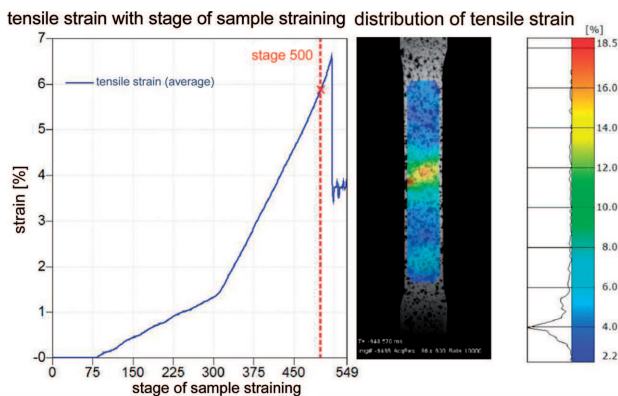


Fig. 5. Exemplarily strain evaluation by ARAMIS at  $0.1 \text{ m}\cdot\text{s}^{-1}$  – Tensile strain with stage/Distribution of tensile strain in measurement area

The left side of Figure 5 displays the change of tensile strain with the following stages of sample straining, where

every stage represents one picture taken by the high speed camera. The amount of tensile strain of each stage is calculated by determination of the average tensile strain of all pixels of the actual picture. The right side of Figure 5 is showing the calculation area in which the determination of tensile strains takes place by the ARAMIS software. It shows the actual stage which is marked in the left side of the figure by the vertical, red line (stage 500). The adiabatic shear band in the middle of the gauge length can be recognized. In this area the maximum plastic strains are determined to around 18.5%, where the average tensile strain of the gauge length is determined to around 6%. For the calculation of stress-strain curves, ILK used the average tensile strains within the gauge length. These average strains tend to correlate with strains that are determined between two points in the gauge length, which would be comparable to the method of measuring strains with incremental extensometers.

Figure 6 shows the comparison of both methods of determining the tensile strains at one test exemplarily. The left side of the figure shows the calculated tensile strains in the gauge length and the determination area which defines the region of interest for determining the average strains. Also the two points between which the elongation of the specimen's surface is calculated is displayed in this part of the image. These points are set with an unstrained distance of 50 mm. The left side of Figure 6 displays the results related to each calculation method. It can be seen that both curves are nearly equal until a significant amount of plastic deformation and shear banding are taking place. Total elongation differs for about 0.4% depending on the measurement method used. Total elongation calculated from the average tensile strains is about 6.7%, and total elongation obtained from the gauge length measurements about 7.1%.

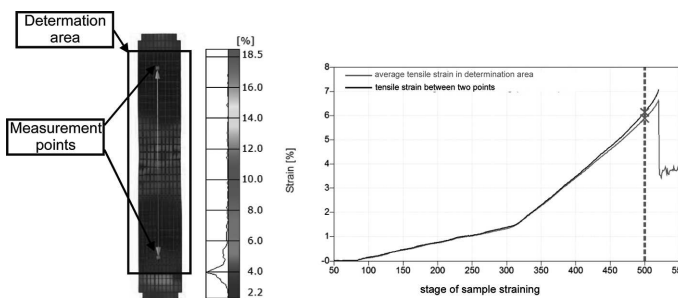


Fig. 6. Calculation methods for strain determination – field measurement vs. line measurement

For the calculation of the stress-strain-curves the strains were calculated from the average tensile strains in gauge length of the sample. Therefore the total elongations tend to be smaller as compared to the results achieved by “classical” strain measurement devices like incremental extensometers.

The chosen examples of stress-strain relationships obtained from the tensile tests are shown in Figure 7. Table 2 summarizes the values of the fracture strength (FS), elastic modulus (E) and total strain to fracture (TSF) for each tested specimen.

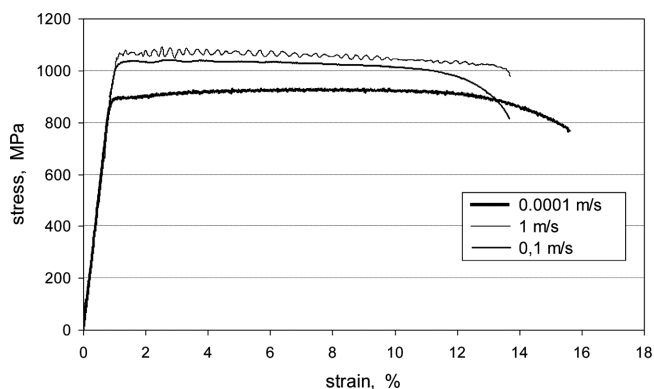


Fig. 7. Stress-strain curves for Ti-6Al-4V alloy tested in tension at various strain rates

The tensile tests performed on Ti-6Al-4V alloy under dynamic conditions showed higher values of the fracture strength of the test samples in comparison to the fracture strength of the samples tested under quasi – static conditions (Fig. 5, Table 2). An increase of the tensile test strain rate resulted in the fracture of the samples at lower value of the total strain, although observed differences were not considerable (Table 2). Moreover, the changes of the tensile tests strain rate did not influence the elastic modulus of the investigated material significantly (Table 2).

TABLE 2

Mechanical properties of Ti-6Al-4V alloy determined in tensile tests

testing velocity $\text{m}\cdot\text{s}^{-1}$	FS MPa	E GPa	TSF %
0.0001	940	103	15.6
0.1	1045	104	12.5
1	1078	104	11.0

#### 4. Metallographic investigations

The fracture surfaces of the samples after tensile tests were examined on Hitachi S3500N scanning electron microscope. Figure 8 shows tensile fracture surfaces of Ti-6Al-4V alloy.

Most of the fracture surfaces exhibit dimples which are indicative of ductile rupture. It should be expected, that fracture nucleates in the area of  $\alpha$  phase nucleation, then plastic flow occurs in the areas of  $\beta$  phase – much more ductile, close to  $\alpha$  phase areas. Figure 8 e,f shows the fracture surface of different character, in which local friction between two areas of previously formed fractures occurred during straining the investigated sample in tensile test. An increase of tensile test strain rate resulted in greater number of the areas in which plastic flow occurred. This observation can signify, that increasing the strain rate leads to decreasing the number of fracture nucleuses as well as decreasing the rate of their propagation.

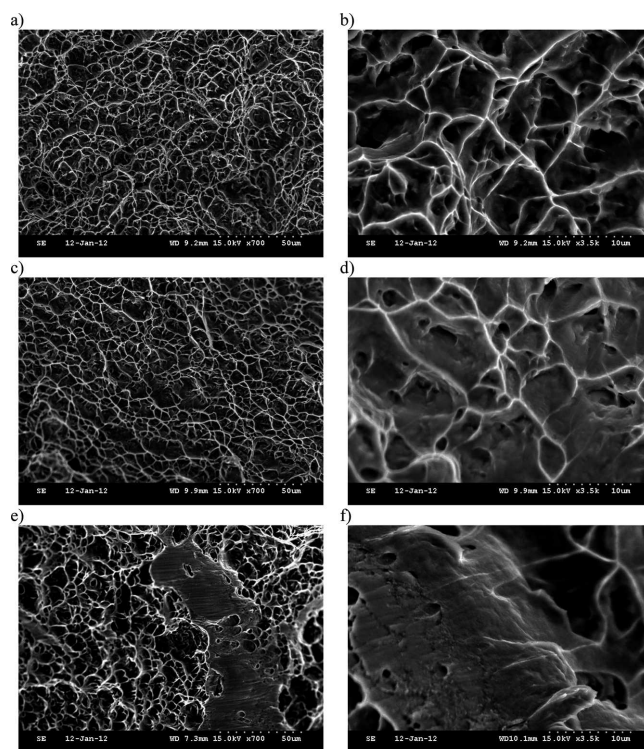


Fig. 8. Tensile fracture surface of Ti-6Al-4V alloy deformed with various testing speeds: a, b)  $0.0001 \text{ m}\cdot\text{s}^{-1}$ ; c, d)  $0.1 \text{ m}\cdot\text{s}^{-1}$ ; e, f)  $1 \text{ m}\cdot\text{s}^{-1}$

#### 5. Conclusions

Basing on the results of investigations of the quasi-static and dynamic tensile properties of Ti-6Al-4V alloy the following conclusions can be drawn:

- The tensile tests performed on Ti-6Al-4V alloy under dynamic conditions showed higher values of the fracture strength of the test samples in comparison to the fracture strength of the samples tested under quasi – static conditions.
- An increase of the tensile test strain rate resulted in the reduction of the values of total strain to fracture for the investigated samples.
- The changes of the tensile tests strain rate did not influence the elastic modulus of the investigated material significantly.
- The fracture surfaces of the majority of the tested samples exhibit dimples which are indicative of ductile rupture.
- Different character of the fracture surface of the sample tested at highest strain rate can be connected with local friction between two areas of previously formed fractures occurred during straining the investigated material in tensile test. An increase of tensile test strain rate resulted in greater number of the areas in which plastic flow occurred. This observation can signify, that increasing the strain rate leads to decreasing the number of fracture nucleuses as well as decreasing the rate of their propagation.
- The results of the performed investigations can be useful in the design of Ti-6Al-4V alloy structural parts operating under high strain rate conditions, in particular for aircraft or aerospace industry applications.

### Acknowledgements

Financial support of Structural Funds in the Operational Programme – Innovative Economy (IE OP) financed from the European Regional Development Fund – Project WND-POIG.01.03.01-12-004/09 is gratefully acknowledged.

### REFERENCES

- [1] M.J. Donachie Jr., (Ed.), Titanium and Titanium Alloys Source Book; American Society of Metals; Metals Park, OH, 265-269 (1982).
- [2] S.L. Semiatin, V. Seetharaman, I. Weiss, Flow behavior and globularization kinetics during hot working of Ti-6Al-4V with a colony alpha microstructure; Mater. Sci. Eng. **A263**, 257-271 (1999).
- [3] P.D. Nicolaou, S.L. Semiatin, Effect of Strain-Path Reversal on Microstructure Evolution and Cavitation during Hot Torsion Testing of Ti-6Al-4V; Metal and Mat. Trans. **A 38**, 3023-3031 (2007).
- [4] R.M. Miller, T.R. Bieler, S.L. Semiatin, Flow softening during hot working of Ti-6Al-4V with a lamellar colony microstructure; Scr. Mater. **40**, 1387-1393 (1999).
- [5] J. Luo, M. Li, W. Yu, H. Li, Effect of the strain on processing maps of titanium alloys in isothermal compression; Materials Science and Engineering **A 504**, 90-98 (2009).
- [6] E.B. Shell, S.L. Semiatin, Effect of initial microstructure on plastic flow and dynamic globularization during hot working of Ti-6Al-4V; Metall. Mater. Trans. **A 30**, 3219-3229 (1999).
- [7] T. Furuhashi, B. Poorganji, H. Abe, T. Maki, Dynamic Recovery and Recrystallization in Titanium Alloys by Hot Deformation; JOM **59**, 1, 64-67 (2007).
- [8] Y.V.R.K. Prasad, T. Seshacharyulu, S.C. Medeiros, W.G. Frazier, A study of beta processing of Ti-6Al-4V: Is it trivial?; J. Eng. Mat & Technol. **123**, 3, 355-360 (2001).
- [9] T. Seshacharyulu, S.C. Medeiros, W.G. Frazier, Y.V.R.K. Prasad, Hot working of commercial Ti-6Al-4V with an equiaxed  $\alpha$ - $\beta$  microstructure: materials modeling considerations; Mater. Sci. Eng. **A284**, 184-194 (2000).
- [10] A. Łukaszek-Sołek, T. Śleboda, J. Krawczyk, P. Bała, M. Wojtaszek, The analysis of forging of Ti-6Al-4V alloy under various thermomechanical conditions; in: Proc. 14th international conference on Metal Forming; Wiley-VCH Verlag GmbH & Co. KGaA, (Steel Research International; spec. ed.), Krakow (2012), 139-142.
- [11] G.A. Salishchev, S.V. Zerebtsov, S.Yu. Mironov, S.L. Semiatin, Formation of grain boundary misorientation spectrum in alpha-beta titanium alloys with lamellar structure under warm and hot working; Materials Science Forum **467-470**, 501-506 (2004).
- [12] W. Hufenbach, A. Langkamp, A. Hornig, C. Ebert, Experimental determination of the strain rate dependent out-of-plane shear properties of textile-reinforced composites; 17th European Conference on Composite Materials (ICCM 17), Edinburgh 2009.
- [13] C. Ebert, W. Hufenbach, A. Langkamp, M. Gude, Modelling of strain rate dependent deformation behaviour of polypropylene; Polymer Testing **30**, 183-187 (2011).
- [14] D.A. Serban, G. Weber, L. Marsavina, V.V. Silberschmidt, W. Hufenbach, Tensile properties of semi-crystalline thermoplastic polymers: Effects of temperature and strain rates; Polymer Testing **32**, 413-425 (2013).